POWER QUALITY IMPROVEMENT BY USING ADAPTIVE QUADRATURE-COMPLEX VARIABLE FILTER BASED ON FOPID CONTROLLER

Sanepalle Gopal Reddy[1] B. Vinnela[2] B. Rishikesh[3] K. Nishkala Priya4, V.Akhil[5]

[1]Associate Professor, Department of EEE, Jyothishmathi Institute of Technology and Science, Nustulapur, Karimnagar, TS, India

[2,3,4,5]UG students, Department of EEE, Jyothismathi Institute of Technology and Science, Nustulapur, Karimnagar, TS, India

Abstract:

Using an adaptive quadrature-complex variable filter based on a fractional-order PID (FOPID) controller, this study aims to improve power quality. Using a FOPID-based control approach, this paper investigates an adaptive quadrature-complex variable filter (AQ-CVF). An effective way to minimize and enhance power quality for different nonlinear loads connected at the Point of Common Interconnection (PCI) is to use grid-interfaced solar photovoltaic (PV) and battery energy storage (BES) systems. An key function of the bidirectional converter (DBC) is to tell the BES to keep critical loads powered even when the RES's output is insufficient. The study also highlights the potential operational issues that may develop as a result of changes in the input and output power of the HSWGIS, which stands for hybrid solar PV-wind -BES linked grid internetwork. In order to evaluate the control mechanism's suitability for the PV-BES grid interfaced system, we provide several static and dynamic modes of operation. The Perturb and Observe (P&O) method and a boost converter (BC) collaborate to maximize the use of renewable energy sources. Examining HSWGIS's performance allows us to validate the efficacy of control approaches in different operational contexts.

Keywords: Power Quality, Adaptive Quadrature-Complex Variable Filter(AQ-CVF), Fractional Order PID (FOPID) Controller, Battery Energy Storage (BES)

I.INTRODUCTION

The growth of renewable energy (RE) sources has been fueled by the increasing demand for power in the modern world. These sources then contribute to the creation of the energy matrix [1]. Renewable energy sources, such as solar photovoltaic (PV) generating, have lately seen a surge in popularity [2]. Power imbalances occur when the unpredictability of power input from solar PV arrays disrupts microgrid operations. The power fluctuations of the RES could be mitigated by the use of a battery energy storage system (BES) [3]. According to Prakash et.al. [4], there should be a renewable energy grid that can stand on its own. Power generation for loads is accomplished by this system by the integration of photovoltaic (PV), wind, and battery energy storage (BES). The wind-photovoltaic hybrid system proposed by Basaran1 et al. [5] may function either standalone or in tandem with the grid, depending on the load. Grid inverters, when operated in dual mode, link the grid to renewable power sources, guaranteeing that essential loads will keep receiving power even when the grid goes down. Alternatively, grid-interfaced hybrid wind-PV-BES systems have the potential to meet load demand while also recharging the grid from surplus electricity. Nevertheless, the system's power quality is significantly

affected by nonlinear loads and variations in solar PV production. Damageful harmonics are produced by nonlinear loads that use power electronics, including electrical drives, LED drives, switch mode power supply (SMPS), and many others. Modifications to When loads are connected at the Point of Common Interconnection (PCI), the grid current harmonic profile takes place. It has dual function as a power quality conditioner and a grid-side converter, converting DC power to AC power.. One load-following capability that a grid-connected hybrid RES system may provide is reactive power and harmonic correction, made possible by its robust control technique [6]. But several adjustments are added to the grid to make it work better while keeping its THD value within the allowed range. Consequently, a trustworthy method for harmonic correction in grid-interfaced RES-based systems is crucial for supplying the grid with high-quality electricity under all operational conditions. Inverter integration is the primary focus of grid-interfaced RES system control, which disregards the integration of solar power and the quality of grid electricity. The two primary methods that grid synchronization is currently implemented are instantaneous reactive power theory [8] and synchronous reference frame theory [7]. is managed. Several sources have indicated that it has been enhanced and changed. Because this concept is always developing, regulating it is a time-consuming and tedious process. In their study on renewable energy grid integration, Rinaldi et al. [9] introduced a regulation of VSCs based on a sliding mode of higher order. On the other hand, monitoring the maximum power point or power quality was not addressed. This collection of blocks is responsible for transforming the single-phase α-β into d−q. When it comes to grid reference generation, PV electricity is already accessible and not dependent on the load current weight. According to this rule, the PV power takes center stage, while the load takes a back seat. Controllers for grid-connected inverters often use complex variable filters (CVFs), frequency lock loops (FLLs), and quadrature signal generators (QSGs) to eliminate harmonics and produce signals perpendicular to the grid voltage [10], [11], and [12], respectively. The authors of [13] calculate the grid voltage's frequency and amplitude by first creating an orthogonal signal using a second-order generalized integral (SOGI) approach. It is already set to the regular grid frequency, which weakens any remaining frequency signals, which is why it doesn't function well with large frequency changes. It is possible to cascade a integral of the second order to SO-SOGI, as mentioned in [13]. This study used a hybrid of a complex variable filter (CVF) and an adaptive quadrature filter to estimate the basic current signal from the load current [14]. The AQ-CVF may be used to extract the basic current signal from non-sinusoidal load current, regardless of whether the reference grid current production is linear or not. In this scenario, the dynamic performance and filtering response may be improved by combining an AQF approach with a CVF control. To address power factor and harmonics, a multi-objective control based on AQ-CVF may be used in a hybrid solar PV-wind -BES linked grid interfaced system (HSWGIS). This is achieved by removing harmonics from the load current and reducing distortion in the grid current., a single voltage source converter (VSC) lessens the power grid's vulnerability to wind speeds and solar radiation fluctuations. The multi-functional capabilities offered by AQ-CVF-based coordinated control go beyond reactive power compensation and include active power distribution among the grid, PCI-connected loads, and the battery, as well as continuous power quality during all system operations..

II. LITERATURE SURVEY

[1] In the 2019 issue of IET Generation, Transmission & Distribution, the authors S. K. Sahoo, N. K. Kishore, and A. K. Sinha discuss "Multi-mode control and operation of a self-sufficient multi-microgrid system" (vol. 13, no. 12, pp. 2550–2562).

Three separate microgrids make up this ring-type system, and they all get their power from the same source: a static synchronous compensator, wind turbines AND solar panels. In case of an emergency, a set of batteries may be used as a backup power supply. Each MG has a voltage-source converter and is connected to both the grid and other MGs. Incorporating a more refined proportional sliding-mode control technique into the system's primary control might improve its power quality in both balanced and unbalanced loading scenarios. To bring the negative-sequence voltage down even lower than the inverter's output voltage, an extra negative-sequence controller is included. In its linked, island, or grid-connected modes of operation, the multi-MG (MMG) system can manage both balanced and unbalanced loads. By using hysteresis characteristics, a sliding-mode system controls the bidirectional DC-DC converters at the DC link, which connect the batteries. This research compares the proposed inverter main control to three other current controllers: proportional-integral, quasi-proportional-resonant, and hysteresis-band current. Both total harmonic distortion and voltage imbalance factor are enhanced by the proposed method as compared to the traditional control strategy.

[2] "Robust Nonlinear Controller Design for On-Grid/Off-Grid Wind Energy Battery-Storage System," published in the November 2018 issue of the IEEE Transactions on Smart Grid, by B. Housseini, A. F. Okou, and R. Beguenane.

One robust nonlinear multi-input-multi-output controller for a wind energy battery storage system is the subject of this article's design process analysis. You have the choice to run the system either on its own or in cooperation with the grid. The controller equations are obtained by a process known as feedback linearization control design.The proposed control approach is an improvement over the existing ones as it eliminates the need for several mode-dependent controllers. The novel approach uses a controller to optimize battery performance for backup power or adding more wind energy storage while minimizing grid contribution. The current approaches for dc-link management use grid-side converters to regulate the load power and dc-link voltage; this methodology uses a bidirectional buck-boost dc/dc converter. To ensure the recommended controller can withstand a range of loads, including dynamic and imbalanced ones, we run simulations of them.

[3] Paper published in April 2013 in the IEEE Transactions on Sustainable Energy by X. Li, D. Hui, and X. Lai titled "Battery Energy Storage Station (BESS)-Based Smoothing Control of Photovoltaic (PV) and Wind Power Generation Fluctuations" (vol. 4, no. 2, pp. 464-473).

The most common and efficient method of making renewable energy sources, including solar and wind, less Aim is to set up a BESS, which stands for battery energy storage system. Levels of power production and battery SOC may be efficiently controlled by BESS-dependent hybrid power systems with the correct management approach. The study reveals the findings of a simulation analysis of a power system that uses wind, PV, and BESS (battery energy storage systems). Goals include improved control of battery SOC and more stable

output from hybrid systems combining wind, solar, and energy storage batteries. A smoothing control approach is proposed for normal-condition battery management and to decrease power fluctuations in the output of wind/photovoltaic hybrids. And we propose a novel way to utilize BESS for real-time power allocation.

[4] Article published in the December 2016 issue of the IEEE Journal of Emerging and Selected Topics in Power Electronics by S. L. Prakash, M. Arutchelvi, and A. S. Jesudaiyan titled "Autonomous PV-Array Excited Wind-Driven Induction Generator for Off-Grid Application in India" (pp. 1259–1269).

The reliability of hybrid wind-solar systems in delivering electricity to off-grid locations depends on their ability to self-propel and use only renewable energy sources. The article outlines a less complicated method of operating a wind-powered induction generator (IG) that uses energy from a standalone hybrid photovoltaic (PV) array, while considering a three-phase variable demand that could be unbalanced or not. To replace the costly permanent magnet synchronous generator often employed in small, standalone wind turbines, the proposed design takes use of the IG's affordability and endurance. Any autonomous system that uses batteries to operate must have the batteryless mode of operation, which is detailed in the article. Having said that, the system should keep running in the event that the batteries die. For this reason, we double-checked the control strategy using hardware and simulation. We used weather stations, wind turbine simulators with 2.2 kW output, and solar panels with 2.4 kW output to carry out comprehensive field testing.

[5] The article "Energy management for on grid and off grid wind/PV and battery hybrid systems" was published in the International Journal of Renewable Power Generation on December 4, 2017, and was written by K. Basaran, N. S. Cetin, and S. Borekci.

There has been a lot of development in renewable energy systems that are either independent or linked to the grid, such photovoltaic (PV) and wind energy systems. This is a concern, especially for small powerful systems, since the inverter market is limited. Many energy systems include inverters, which may function either on or off the grid. The construction of a wind-PV hybrid system that can operate both independently and in conjunction with the grid is a new approach to power management that has been developed in this study. The inverter used in this study can function both when connected to and when disconnected from the grid. Gel batteries are used in the hybrid system since energy is continuously needed. An efficient movement of energy between batteries, loads, and the grid is provided by the newly-developed Power Management Unit, which measures data from various locations in the system. An efficiency boost of up to 10% is possible with the newly designed control unit.

III. PROPOSED System configuration

The structure of HSWGIS is shown in Figure 1. Using DC-DC boost converters (BC), two renewable energy sources—wind and solar PV—are linked to a common DC link voltage, or Vdc. The employment of permanent magnets in a brushless DC generator is one method of converting wind energy into usable power. Connected in series with the unregulated rectifier are nonlinear loads, such the R-L load. The on/off switching of the VSC produces high-frequency current harmonics, which are attenuated by a low-frequency bridge inductor (Lfb) and then eliminated by an The R-C ripple filter is attached to the PCI pin. Through a bidirectional converter, a pair of wires transport the DC link voltage, Vdc, from the BES unit.

A DC link is controlled by the management of BDC charging and discharging. The need for the BES unit to store the extra photovoltaic power (PPV) produced by the PV array becomes apparent as the voltage drop increases. The μ-grid operates autonomously in case of a fault.

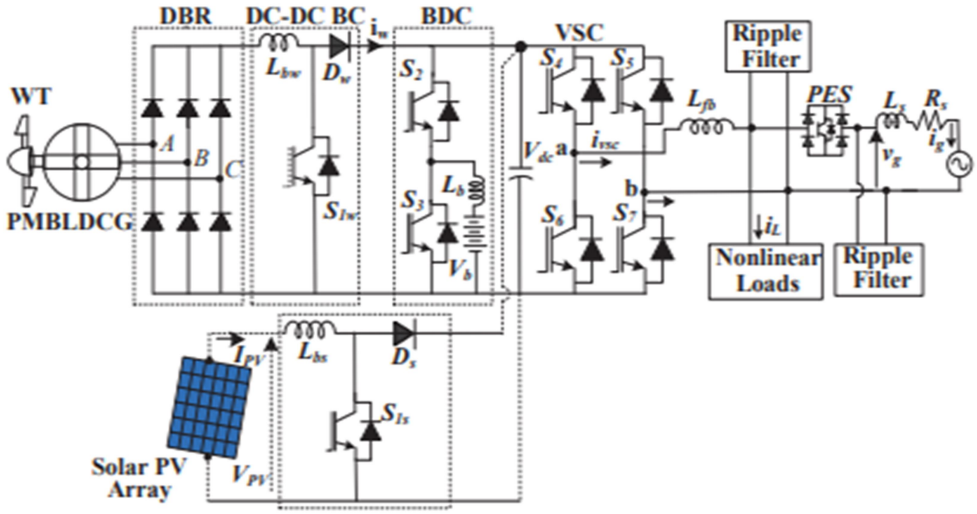

Fig. 1. System configuration

II. CONTROL DESIGN

A. Switching Control of VSC

In Figure 2, we can see the v-grid that combines PV, wind, and BES, and it's controlled by many objectives. Here we detail the algorithm's design and how it deals with discretion.

B. Switching Control of VSC

To regulate the switching of grid-interfaced VSCs, the PV-wind BES based v-grid was equipped with the AQ-CVF current control system, as shown in Figure 2. Multistructural AQ-CVF switching controls the grid-interfaced VSC to provide sinusoidal waveform grid current. To mitigate the impact of unknown harmonics and disturbances on grid current, the AQ-CVF filter was developed. By eliminating nonlinearities using the AQ-CVF, the fundamental frequency component of finding the load current is possible. To enhance the power of the system, grid current control aims to increase the frequency of gate pulses. quality.

1) Development of AQF (Adaptive Filter)

After removing the harmonics from the load current, the AQF may be utilized to determine the relevant component. Figure 2 depicts the AQF's design. Some background on the AQF -regulating equations is given below [14]:

(1)

$$i_\beta(s) = \frac{1}{s}[K_{\beta 1}[-i_\beta(s) + \omega_o i_\alpha(s)]$$

(2)

The transfer functions of AQF [14] may be estimated using equations (1) and (2) as

$$\frac{i_\alpha(s)}{i_L(s)} = \frac{K_\beta(s+1)}{s+(K_\beta+1)s+(K_\beta+\omega_o^{\,2})} \quad (3)$$

$$\frac{i_\beta(s)}{i_L(s)} = \frac{K_\beta\omega_o}{s+(K_\beta+1)s+(K_\beta+\omega_o^{\,2})} \quad (4)$$

Kβ is the symbol for the AQF's gain. The load current's in-phase (iα) and quadrature-phase (iβ) components signal are computed in accordance with the AQF.

2) Development of CVF (Complex Variable Filter)

See the basic building blocks of the adaptive variable filter in Figure 2. The expression of the single-phase current component under the αβ reference frame is determined by the AQF control, as mentioned in (3) and (4), and this control is essential for constructing the CVF structure. The solution of equations (3) and (4) may provide a fundamental, distortion-free, sinusoidal component of the reference current. Integrating the current signals α−H generated by the AQF is crucial for obtaining the CVF's transfer function [12].

$$G(s) = \frac{i_{\alpha\beta g}(s)}{i_{\alpha\beta}(s)} = \frac{s+j\omega}{s^2+j\omega^2} \quad (5)$$

$$\text{Where, } I_{\alpha\beta}(t) = e^{j\omega t}\int e^{-j\omega t} i_{\alpha\beta g}(t)\,dt \quad (6)$$

If the phase delay is zero and ϋ=ϋc, you may set the TF magnitude to 1 by meticulously choosing the amount of gain K in G(s). Alternately, improving CVF performance is achieved by decreasing the transient length and increasing the adaptive gain, K. This is why we adjust the adaptive gain, K, in a way that The filter shortens transient duration and gets rid of phase delay by isolating the distortion-free basic current component [12].

$$G(s) = \frac{i_{\alpha\beta g}(s)}{i_{\alpha\beta}(s)} = K\frac{(s+K)+j\omega}{(s+K)+\omega^2} \quad (7)$$

In the α-β frame, the load current signals vα and vώ, as well as the basic load current components iűg and iĶg in the output signal iǫĶg, may be used to formulate the following formula [12].

$$i_{\alpha g}(s) = \frac{K}{s}[i_\alpha(s) - i_{\alpha g}(s)] - \frac{\omega}{s} i_\beta(s) \quad (8)$$

$$i_{\beta g}(s) = \frac{K}{s}[i_\beta(s) - i_{\beta g}(s)] - \frac{\omega}{s} i_\alpha(s) \quad (9)$$

In the α-β plane, namely in the in both the in-phase and quadrature-phase directions, the primary component of the load current is represented by the filter's output.

3) Calculation of PCI Voltage and Unit Templetes

Thanks to equations (5.3) and (5.4), the AQ-CVF determines the vg's in-phase and quadrature phase grid voltages, respectively. One may determine the magnitude of the terminal voltage, Vt, using the approach, and it is

$$V_t = \sqrt{(v_{\alpha g}^2 + v_{\beta g}^2)} \quad (10)$$

Here are the estimated unit templates:

$$u_p = \frac{v_{\alpha g}}{V_t},\ u_q = \frac{v_{\beta g}}{V_t} \quad (11)$$

Up represents the voltage in-phase template and uq represents the voltage quadrature phase template when the grid is synchronized.

4) Feed-Forward Terms of Wind and Solar

Integrating PV power feed-forward with wind feed-forward may make the v-grid more responsive in real-time. This IPVFF, when aggregated, is

$$I_{PVFF} = \frac{2P_{PV}}{V_t} \quad (12)$$

The IWFF is estimated as,

$$I_{WFF} = \frac{2P_w}{V_t} \quad (13)$$

5) Reference Grid Current Estimation

By estimating the reference grid current using the AQ-CVF based current control, the switching pluses of VSC may be enhanced. According to Figure 2, the sample and hold (S&H) blocks and quadrature template of the PCI voltage are used to ascertain the maximum value of the basic load current (Id), which is accessible at the AQ-CVF output.

Our best guess is that the reference grid current's net peak component is

$$I_{dr} = I_d - I_{WFF} - I_{PVFF} \quad (14)$$

Multiplying the in-phase unit template (up) by the projected value of Idr yields the reference current.

$$i_{gref} = I_{rd} * u_p \quad (15)$$

As shown, It is possible to anticipate VSC switching pulses using the hysteresis switching controller in conjunction with the difference between ig and igr.

$$i_{egr} = i_{gref} - i_g \quad (16)$$

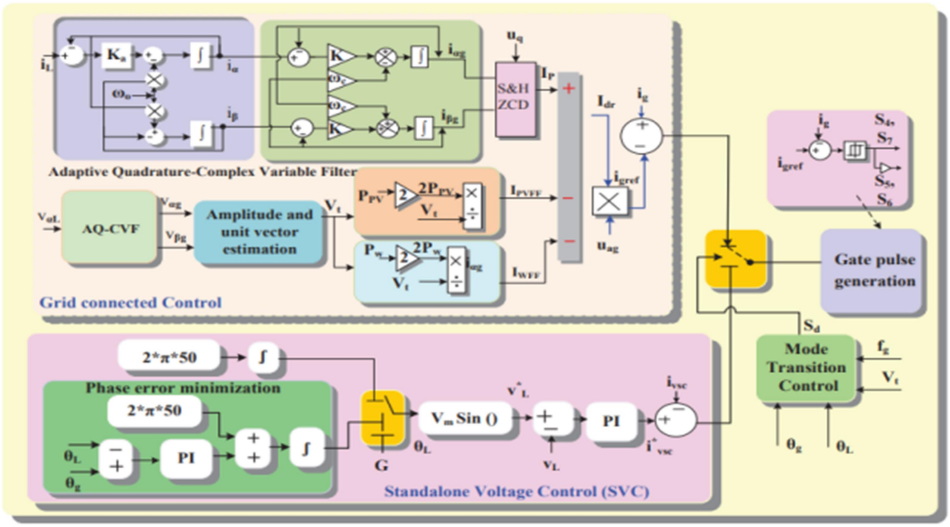

Fig. 2. Control scheme of solar PV–wind BES based AC µ-grid

6) Standalone Mode

Power to the grid and the PCI is interrupted by the SSS when the main grid cutoff is not present, and the VSC enters voltage control mode.. Even when disconnected from the grid, the system keeps running because to the VSC's ability to change the amplitude and frequency of the PCI voltage. In this scenario, when there is no external input, we use the reference frequency to get the instantaneous phase of the reference load voltage. The goal of VSC control is to keep vL where it should be. A PI controller compares the detected vL to the reference value v* L to obtain the reference VSC current i* VSC. The calculated reference current i* vsc may be compared to the VSC current to help bring the inaccuracy down. In autonomous mode, the VSC pulses are produced by the hysteresis switching control in response to the ensuing error.

7) DC-DC Bidirectional Converter

When renewable energy sources and load demand are not in sync, the BES unit steps in to fill the gap. On display in Figure 1 is an AC-DC converter that can move current in both directions. The DC-DC bidirectional converter controls the flow of electricity by means of its efficient switching. BES receives or uses. It is crucial to charge and discharge the BES appropriately in order to maintain a balanced power grid. Two cascaded PI controllers make up the converter control loop, which responds to system changes by keeping the voltage drop (Vdc) and charging current (Ibat) constant.

8) Boost Convertor Control for Solar PV Array

Because the PV array is nonlinear and solar insolation fluctuates stochastically, it is essential to calculate the boost converter's duty cycle using a maximum power point tracking (MPPT) control technique (P&O), as shown in Figure 3 (b).

9) Boost Convertor (BC) Control for Wind Energy

If the reference current is compared to the sensed produced DC wind current (iw), the set-point power from the PMBLDC generator provided by the wind turbine may be computed. The procedure is shown in Figure 3(c).

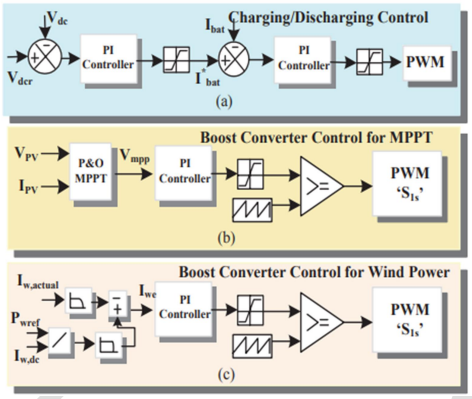

Fig. 3. The DC-DC bidirectional converter's control structure, (b) the boost converter's MPPT voltage control, and (c) the wind power extraction voltage control

IV. PROPOSED FOPID CONTROLLER

Industrial control systems often use PID controllers, which function as a kind of universal feedback control loop. If a consistency process variable deviates too far from the target set point, the PID controller will formulate and execute corrective procedures to restore the process to its intended state. An integer-order PID controller's transfer function looks like this:

$$G_c(S) = K_p + K_s s^{-1} + K_d s \qquad (17)$$

A PID controller relies on two time constants, Kd and Ki, to function. The PID controller algorithm relies on these three factors. All three of the factors listed by the Integral—relative gain, the amount of recent mistakes, and the rate of error change—influence the error response. After you've completed all three steps, you'll be able to use control valves and heating components to regulate a process. The use of PID controllers is shown in Figure 4 for closed loop control systems.

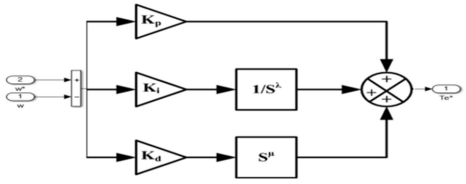

Fig. 4 FOPID controller-based closed-loop process control system.

V.SIMULATION RESULTS

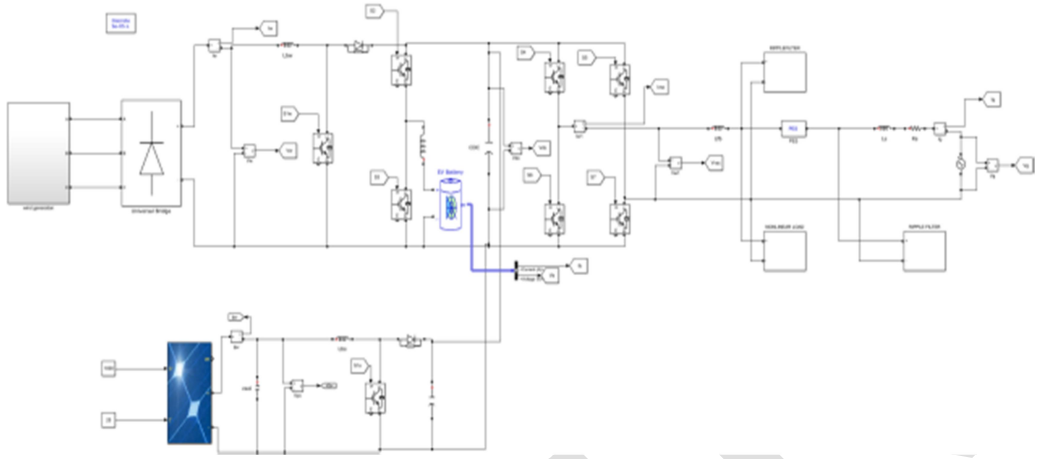

Fig.5 MATLAB/SIMULINK circuit of the system

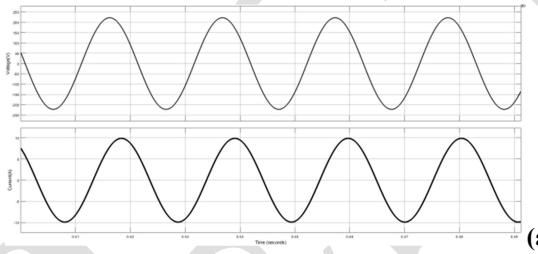

(a)

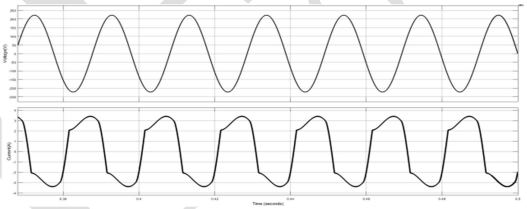

(b)

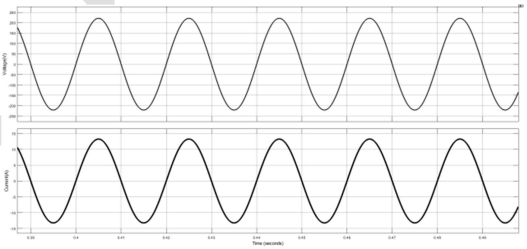

(c)

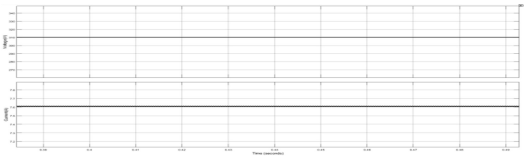

(d)

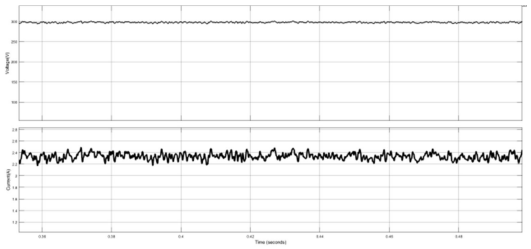

(e)

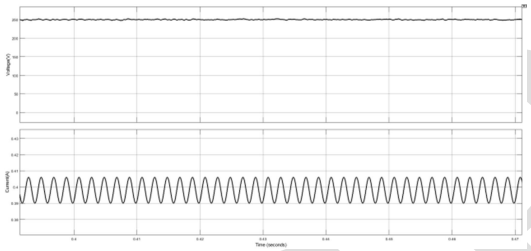

(f)

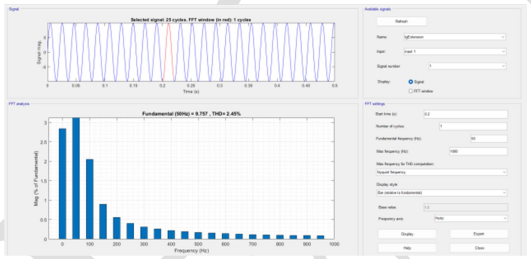

(g)

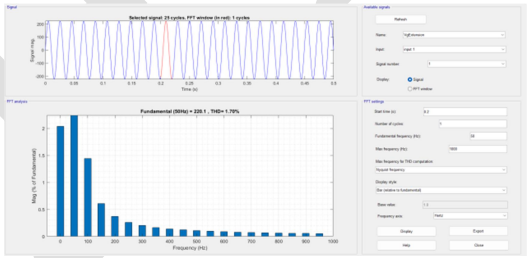

(h)

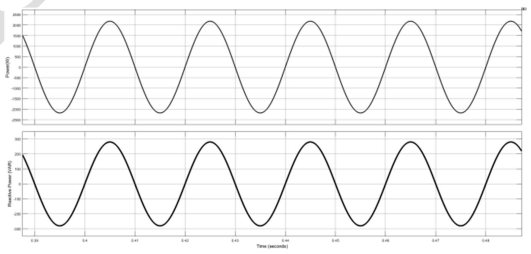

(i)

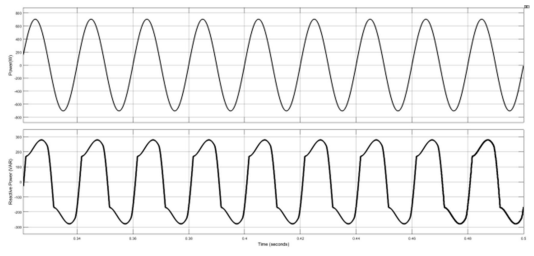

(j)

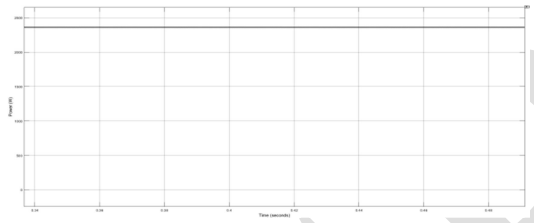

(k)

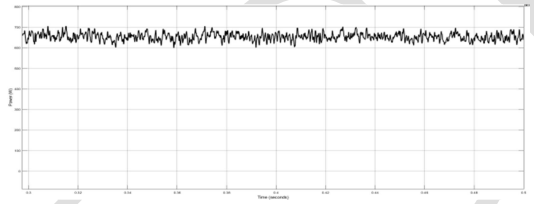

(l)

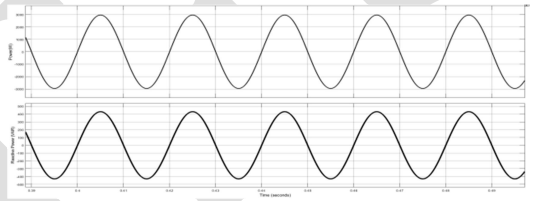

(m)

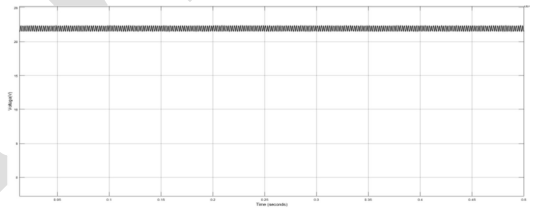

(n)

Fig.6 The findings of the µ-grid system running in grid interfaced mode Pg, PL, PPV, wind power, VSC power, battery power, total harmonic distortion (THD) of ig and vg, iL and vg, iVSC and vvsc, IPV and VPV, wind current and voltage, Ibat and Vbat, and so on are all components of the equation.

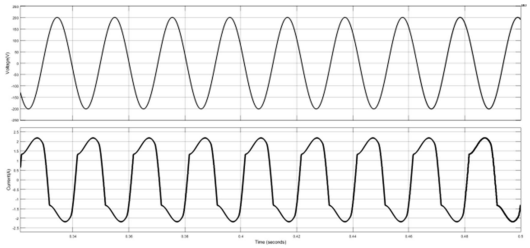

(a)

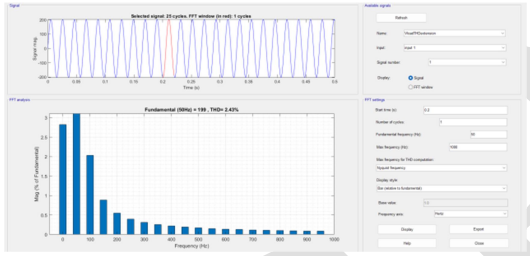

(b)

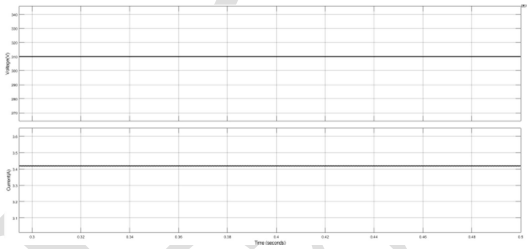

(c)

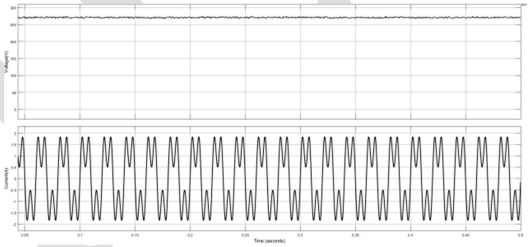

(d)

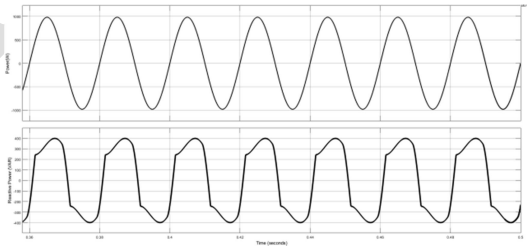

(e)

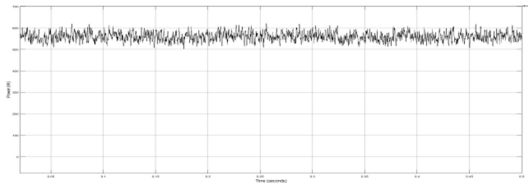

(f)

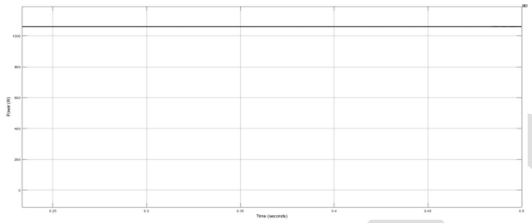

(g)

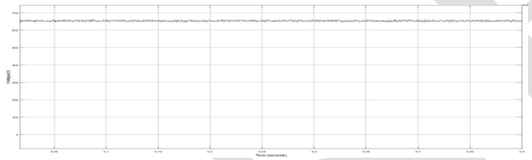

(h)

Fig 7: The µ-grid system's performance in standalone mode (a) VLoad voltage plus current, (b) VLoad voltage with total harmonic distortion, (c) PV current plus voltage (d) Power from the wind, (e) power from the load, (f) power from the wind, (g) power from photovoltaic cells, and (h) power from batteries

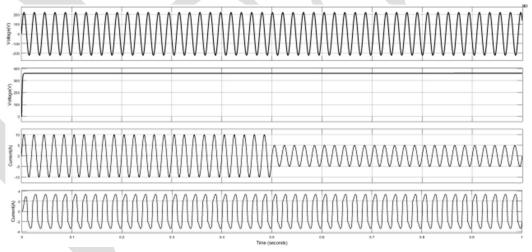

(a)

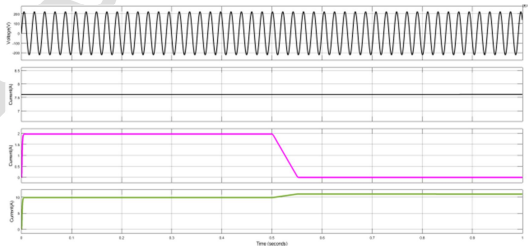

(b)

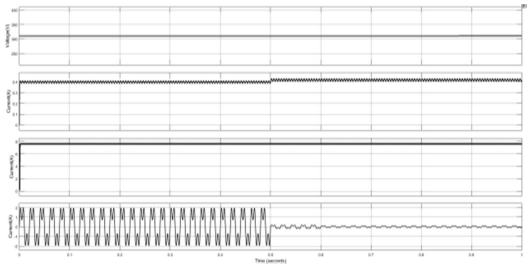

(c)

Fig.8 Dynamic response of the µ-grid system under the variation of renewable

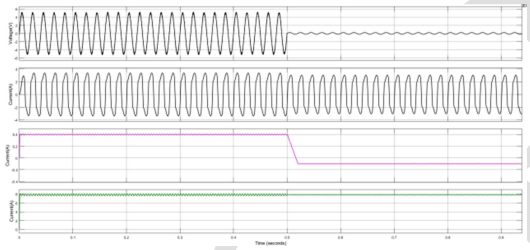

(a)

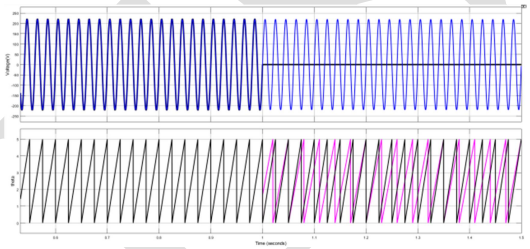

(b)

Fig 9.The performance of HSWGIS while switching from grid interfaced mode to islanding mode, with input voltages vg, vL, Ibat, and IPV, and output voltages vg, vL, QL, and Qg.

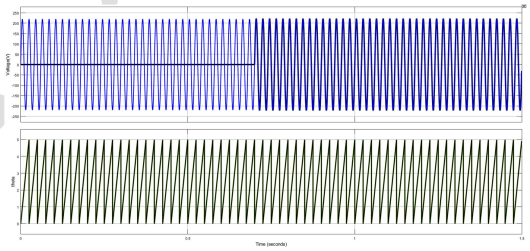

(a)

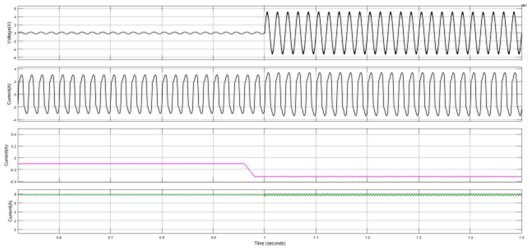

(b)

Fig.10 From islanding mode to grid, the performance of HSWGIS (a) as vg, vL, QL and Qg, and (b) as vg, vL, Ibat and IPV.

COMPARISION TABLE

	Existing	**Extension**
Vg	3.71%	2.45%
Ig	2.21%	1.70%
VLoad	3.64%	2.43%

CONCLUSION

Lots of trials have been run using wind, solar PV, and BES v-grids. The functioning of the μ-grid is validated in several ways via the use of a MATLAB simulation. The v-grid works well in both grid-tied and islanding modes. Mode transitions must be seamless for procedures that include grid synchronization, islanding, or re-synchronization. Using an AQ-CVF with FOPID control technology, power quality concerns were handled and a DC μ-grid that depends on wind BES and solar PV was synchronized. Integrating AQ-CVF with FOPID allows for the elimination of harmonics in both the load and grid side voltages. In order to maintain consistent power quality, this controller adheres to IEEE standard 519. Furthermore, the μ-grid will always have sufficient power to fulfill its demands because to the islanding operating mechanism. A single VSC can link several DC power sources to the grid, like as wind, solar PV, and BES. Reduce the amount of converters used by each solar array, wind turbine, and BES unit and increase the proportion of VSC to make the deployed μ-grid cost-effective.

REFERENCES

[1] S. K. Sahoo, N. K. Kishore and A. K. Sinha, "Multi-mode control and operation of a self-sufficient multi-microgrid system," IET Generation, Transmission & Distribution, vol. 13, no. 12, pp. 2550- 2562, 2019

[2] B. Housseini, A. F. Okou and R. Beguenane, "Robust Nonlinear Controller Design for On-Grid/Off-Grid Wind Energy Battery Storage System," IEEE Trans. on Smart Grid, vol. 9, no. 6, pp. 5588- 5598, Nov. 2018.

[3] X. Li, D. Hui and X. Lai, "Battery Energy Storage Station (BESS)- Based Smoothing Control of Photovoltaic (PV) and Wind Power Generation Fluctuations," IEEE Tran. on Sust. Energy, vol. 4, no. 2, pp. 464-473, April 2013.

[4] S. L. Prakash, M. Arutchelvi and A. S. Jesudaiyan, "Autonomous PV-Array Excited Wind-Driven Induction Generator for Off-Grid Application in India," IEEE Journal of Emerging and Selected Topics in Power Electronics, vol. 4, no. 4, pp. 1259-1269, Dec. 2016.

[5] K. Basaran, N. S. Cetin and S. Borekci, "Energy management for on grid and off-grid wind/PV and battery hybrid systems," IET Renewable Power Generation, vol. 11, no. 5, pp. 642-649, 12 4 2017.

[6] S. Munir and Y. W. Li, "Residential Distribution System Harmonic Compensation Using PV Interfacing Inverter," IEEE Transactions on Smart Grid, vol. 4, no. 2, pp. 816-827, June 2013.

[7] M. Karimi-Ghartemani, "A Unifying Approach to Single-Phase Synchronous Reference Frame PLLs," IEEE Transactions on Power Electronics, vol. 28, no. 10, pp. 4550-4556, Oct. 2013.

[8] Fang Zheng Peng and Jih-Sheng Lai, "Generalized instantaneous reactive power theory for three-phase power systems," in IEEE Transactions on Instrumentation and Measurement, vol. 45, no. 1, pp. 293-297, Feb. 1996.

[9] G. Rinaldi, P. P. Menon, C. Edwards and A. Ferrara, "Higher Order Sliding Mode Observers in Power Grids with Traditional and Renewable Sources," IEEE Control Syst. Letters, vol. 4, no. 1, pp. 223-228, Jan.2020.

[10] P. Rodriguez, A. Luna, I. Candela, R. Mujal, R. Teodorescu, and F. Blaabjerg, "Multiresonant frequency-locked loop for grid synchronization of power converters under distorted grid conditions," IEEE Trans. Ind. Electron., vol. 58, no. 1, pp. 127–138, Jan. 2011.

[11] P. Lamo, F. López, A. Pigazo and F. J. Azcondo, "An Efficient FPGA Implementation of a Quadrature Signal-Generation Subsystem in SRF PLLs in Single-Phase PFCs," IEEE Transactions on Power Electronics, vol. 32, no. 5, pp. 3959-3969, May 2017

[12] X. Quan, X. Dou, Z. Wu, M. Hu and A. Q. Huang, "Complex-Coefficient Complex-Variable Filter for Grid Synchronization Based on Linear Quadratic Regulation," IEEE Transactions on Industrial Informatics, vol. 14, no. 5, pp. 1824-1834, May 2018

[13] Z. Xin, X. Wang, Z. Qin, M. Lu, P. C. Loh and F. Blaabjerg, "An Improved Second-Order Generalized Integrator Based Quadrature Signal Generator," IEEE Tran. on Power Electronics, vol. 31, no. 12, pp. 8068-8073, Dec. 2016.

[14] F. K. d. A. Lima, R. G. Araújo, F. L. Tofoli and C. G. C. Branco, "A Phase-Locked Loop Algorithm for Single-Phase Systems with Inherent Disturbance Rejection," IEEE Transactions on Industrial Electronics, vol. 66, no. 12, pp. 9260-9267, Dec. 2019.